This article was downloaded by:
On: *25 January 2011*
Access details: *Access Details: Free Access*
Publisher *Taylor & Francis*
Informa Ltd Registered in England and Wales Registered Number: 1072954 Registered office: Mortimer House, 37-41 Mortimer Street, London W1T 3JH, UK

Liquid Crystals

Publication details, including instructions for authors and subscription information:
http://www.informaworld.com/smpp/title~content=t713926090

Optical storage in a smectic mesophase: thermal amplification of light-induced chromophore orientations and surface relief gratings

A. Stracke[a]; J. H. Wendorff[a]; D. Goldmann[b]; D. Janietz[b]
[a] Philipps-Universitat Marburg, [b] Universitat Potsdam,

Online publication date: 06 August 2010

To cite this Article Stracke, A. , Wendorff, J. H. , Goldmann, D. and Janietz, D.(2000) 'Optical storage in a smectic mesophase: thermal amplification of light-induced chromophore orientations and surface relief gratings', Liquid Crystals, 27: 8, 1049 — 1057

To link to this Article: DOI: 10.1080/02678290050080805

URL: http://dx.doi.org/10.1080/02678290050080805

PLEASE SCROLL DOWN FOR ARTICLE

Full terms and conditions of use: http://www.informaworld.com/terms-and-conditions-of-access.pdf

This article may be used for research, teaching and private study purposes. Any substantial or systematic reproduction, re-distribution, re-selling, loan or sub-licensing, systematic supply or distribution in any form to anyone is expressly forbidden.

The publisher does not give any warranty express or implied or make any representation that the contents will be complete or accurate or up to date. The accuracy of any instructions, formulae and drug doses should be independently verified with primary sources. The publisher shall not be liable for any loss, actions, claims, proceedings, demand or costs or damages whatsoever or howsoever caused arising directly or indirectly in connection with or arising out of the use of this material.

LIQUID CRYSTALS, 2000, VOL. 27, NO. 8, 1049–1057

Optical storage in a smectic mesophase: thermal amplification of light-induced chromophore orientations and surface relief gratings

A. STRACKE, J. H. WENDORFF*
Institut für Physikalische Chemie und Wissenschaftliches Zentrum für Materialwissenschaften, Philipps-Universität Marburg, 35032 Marburg, Germany

D. GOLDMANN and D. JANIETZ
Fachbereich Chemie und Institut für Dünnschichttechnologie, Universität Potsdam, Kantstrasse 55, 14513 Teltow, Germany

(*Received 11 September 1999; accepted 24 January 2000*)

This contribution is concerned with the exceptionally strong influence of smectic mesophase formation on the optically induced orientation and on the surface relief grating formation in a liquid crystalline melamine derivative containing azobenzene groups. We demonstrate that the strong amplification of optically induced holographic gratings by thermal treatment is not only caused by the enhancement of photo-orientation through the mesophase formation, but is furthermore a consequence of significant amplification of the amplitude of surface relief gratings during the thermal development.

1. Introduction

It is well documented that photo-orientation of azobenzene units is induced through *trans-cis-trans*-isomerization cycles by irradiating liquid crystalline materials containing such chromophores with linearly polarized light [1–9]. The reorientation of the chromophores leads to a significant optical birefringence due to the large anisotropy of the polarizability of the chromophores. Such materials have been considered for digital and holographic optical storage. During recent years the concept has been improved by inserting, in addition, non-photoactive calamitic mesogens into the photosensitive material. In liquid crystalline side group copolymers of this type, the non-absorbing mesogenic group couples to the light-induced reorientation of the azo chromophore through dipolar or steric interactions, as was shown by a combination of UV/Vis- and IR-dichroism studies [10]. This 'cooperative motion' leads to a higher efficiency of the photo-orientation process and thus to an enhancement of the photoinduced birefringence [11, 12].

Of special interest are systems which can be quenched into the amorphous state, for instance, by spin coating. It was discovered that the cooperative interactions lead to a significant amplification of the light-induced optical modulations within the amorphous film by annealing it in a temperature range above the glass transition and below the clearing temperature. This phenomenon, denoted as 'thermal gain effect' was observed for the first time in calamitic side group polymers [13]. In a recent publication we reported that the effect is more general and can also be observed in hybrid materials in which the photoaddressable group (calamitic) and the mesogenic unit (discotic) are of different shape [14].

Up to now the discussion on the mechanism of the thermal gain effect has been limited to the contribution of cooperative reorientation processes to the strong enhancement of the optically induced changes. However, in 1995 Tripathy and co-workers [15] and Natansohn and co-workers [16] discovered that irradiation of azo dye-containing films with an interference pattern of coherent light can induce not only an alignment of the chromophores throughout the volume of the material, but also a controlled modification of the film surface. Hvilsted *et al.* [17] attributed the surface relief grating (SRG) formation in liquid crystalline polymers to the existence of an attractive mean field potential between the mesogenic chromophores. It is assumed that the formation is the consequence of a large scale, photo-induced mass transport in the glassy state of the materials. The formation of SRGs results in a very stable and highly efficient grating. This process may even dominate the contribution of the initially formed refractive index grating originating from a reorientation of the chromophores [18, 19]. Surface modifications, as an additional contribution to the observed signal enhancement during the thermal gain process, have thus to be taken into account.

---

*Author for correspondence.

Liquid Crystals ISSN 0267-8292 print/ISSN 1366-5855 online © 2000 Taylor & Francis Ltd
http://www.tandf.co.uk/journals

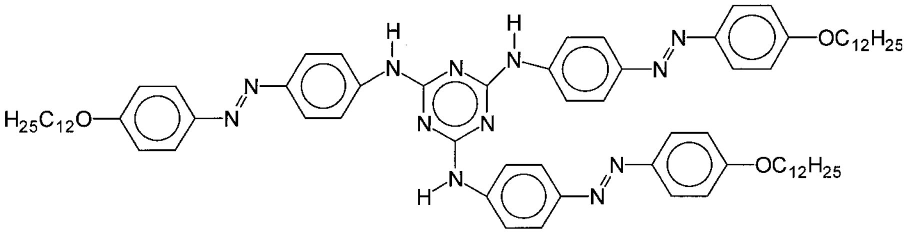

Figure 1. Molecular structure of the smectic trisazomelamine, TAM.

We demonstrate in this paper that the thermal development of a photoinduced grating in a low molecular mass liquid crystal will lead to a strong amplification of the optical signal, and we give evidence that this is due to an induction or enhancement of a periodic surface modulation. The effect is characterized in detail by means of birefringence measurements, holographic grating experiments and surface profile analysis.

2. Experimental procedures

2.1. *Sample preparation*

The investigated liquid crystalline model compound trisazomelamine (TAM) consists of a triazine core, linked to three rod-like azobenzene units bearing a C_{12}-alkyl chain (figure 1).

The compound is isotropic above 239°C and, on cooling, a nematic phase is observed which changes to a smectic phase below 221°C. The synthesis and a detailed characterization of the mesophase behaviour of TAM and a number of homologues have been reported previously [20]. Figure 2 gives an illustration of the structural model of the smectic phase as suggested in [20].

Depending on the cooling rate, both a smectic glassy state state ($T_g = 32°C$) or an amorphous glassy state can be obtained. Amorphous and optically transparent films were prepared by the spincoating technique. These films (with a thickness of 0.4–2 µm) show no detectable birefringence up to 109°C on heating, indicating that the formation of the LC phase is kinetically suppressed up to this temperature.

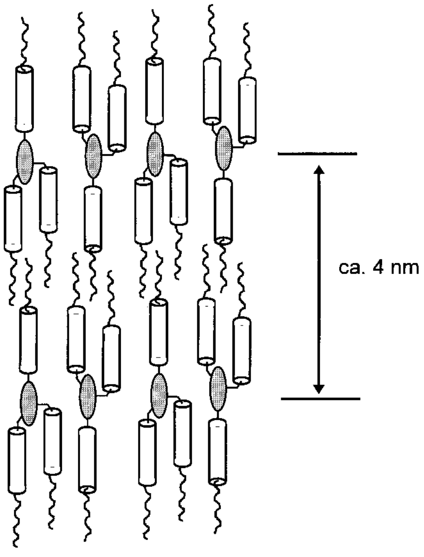

Figure 2. Model of the smectic layer structure for TAM.

2.2. *Optical investigations*

For birefringence and holographic grating experiments we used the identical geometric arrangement of the writing beam and sample position as that sketched in figure 3.

The writing beam propagates in the *z*-direction and is *y*-polarized (s-polarization). We used s-polarized writing beams to minimize the effect of SRG formation during the writing process at room temperature. It is known that s-polarized beams induce only weak or even no surface gratings at least in polymers [21, 22]. It has, however, to be pointed out that the low molecular mass compound TAM shows, even under these conditions, a strong tendency to form surface gratings. The temperature dependence of the light-induced optical changes was investigated by placing the sample inside a heating cell, allowing temperature dependent measurements in the range 25 to 250°C with heating rates between 2 and 500°C h^{-1} and a precision of ± 1°C.

2.3. *Photoinduced birefringence*

In order to study the kinetics of photoinduced reorientation of the azo groups and the influence of temperature on the induced optical changes, we measured the

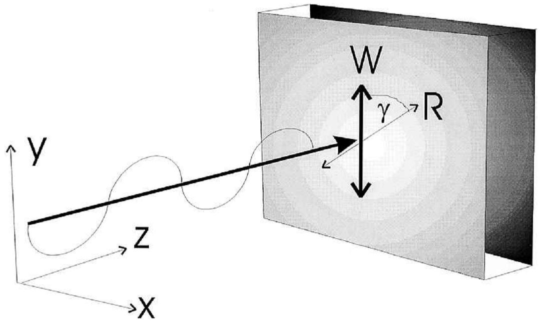

Figure 3. Geometry of the writing process (W = polarization of the writing beam, R = polarization of the probe beam, γ = angle between polarization directions of W and R).

time dependence of photoinduced birefringence under irradiation with linearly polarized light of a cw argon ion laser operating at $\lambda = 488\,\text{nm}$. The birefringence was derived from the intensity of a HeNe probe beam ($\lambda = 633\,\text{nm}$) which passes through crossed polarizers with the sample positioned between the polarizer and analyser (figure 4).

The photoinduced orientation of the rod-like chromophores along a preferred direction causes a phase shift in the probe beam and so it has a non-zero intensity after passing the crossed polarizers. The photoinduced birefringence Δn can then be calculated from the transmitted intensity of the HeNe beam by:

$$\Delta n = \frac{\lambda_{\text{HeNe}}}{\pi d}\left[\arcsin\left(\frac{I}{K_{\text{A}} I_0}\right)^{1/2}\right]. \tag{1}$$

This simple method of determining the photoinduced birefringence is, however, not sensitive to the sign of Δn. By definition, the photoinduced birefringence has a negative sign for the photo-orientation in calamitic systems ($\Delta n = n_y - n_x$, with $n_x > n_y$ after the reorientation is completed). This problem can be overcome by placing a quarter wave plate in the pathway of the probe beam, between the sample and the analyser. The slow axis of this device has to be at an angle of $3/4\pi$ with respect to the polarization direction of the writing beam, and the analyser must be rotated by an angle α relative to the crossed position [23]. The birefringence can then be calculated from the measured intensity of the probe beam by:

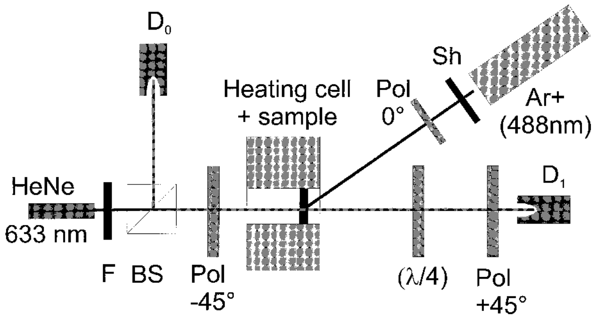

Figure 4. Set-up for the measurement of photoinduced birefringence (Pol = polarizer; Sh = Shutter; F = filter; BS = beamsplitter, $\lambda/4$ = quarter wave plate; D_0, D_1 = detectors).

$$\Delta n = \frac{\lambda_{\text{HeNe}}}{\pi d}\left[\arcsin\left(\frac{\Delta I_\delta}{K_{\text{A}} I_0} + \sin^2\alpha\right)^{1/2} - \alpha\right]$$

$$\text{with } \Delta I_\delta = I(t) - I(t = 0). \tag{2}$$

2.4. *Holographic grating experiments*

The set-up of the holographic grating experiment is sketched in figure 5. Intensity gratings with a grating constant $\Lambda = 5.1\,\mu\text{m}$ were obtained by the interference of two coherent linearly polarized laser beams in the plane of the sample. We used a cw argon ion laser operating at 488 nm. The resulting refractive index modulation

$$n(x) = n_0 + n_1 \cos\left(\frac{2\pi x}{\Lambda}\right) \tag{3}$$

was read out via the diffraction of a HeNe laser beam at 633 nm. The experimentally obtained diffraction efficiency is directly related to the induced refractive index modulation:

$$\eta = \frac{I}{I_0} \approx \sin^2\left(\frac{\pi n_1 d}{\lambda_{\text{HeNe}} \cos\theta_{\text{HeNe}}}\right) \tag{4}$$

which in turn is related to the induced orientational order of the optical axes of the azo dyes.

We employed a polarizing beam splitter and half wave plates in order to achieve equal polarization directions for the writing and reading beams, as well as two writing beams of equal intensity. A motor-controlled half wave plate located in the pathway of the HeNe probe beam allowed the characterization of the grating's anisotropy by rotating the polarization plane of the reading beam

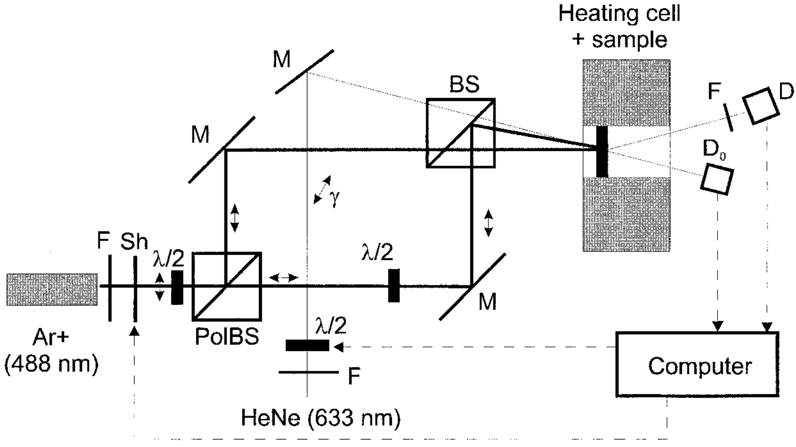

Figure 5. Set-up of the holographic grating experiment (Pol = polarizer; F = filter; Sh = Shutter; BS = beamsplitter; PolBS = polarizing beam splitter; M = mirror, $\lambda/2$ = half wave plate; D_0, D_1 = detectors; the arrows denote polarization directions within the *xy*-plane).

through an angle γ. Moreover, this feature enabled us to calculate the photoinduced birefringence from the diffraction efficiencies in the parallel position of the writing and reading polarization (η_y, $\gamma = 0°$) and in the perpendicular position (η_x, $\gamma = 90°$):

$$\Delta n = 2n_{1,x} + 2n_{1,y}. \quad (5)$$

All film samples investigated belong to the range of thin gratings. Therefore the refractive index changes $n_{1,x}$ and $n_{1,y}$ can be calculated from the diffraction efficiencies by using the following equation, which is derived from the Bessel function, describing thin gratings [24]:

$$2n_1 \approx \frac{\lambda_{\mathrm{HeNe}}}{\pi d} 1.171 \arcsin(1.7185\sqrt{\eta}). \quad (6)$$

2.5. *Surface profile analysis*

The surface profile measurements were performed with a Dektak profile analyser (Dektak3ST, Veeco) and an atomic force microscope (AFM, SA 1/BD 2, Park-Scientific Instruments).

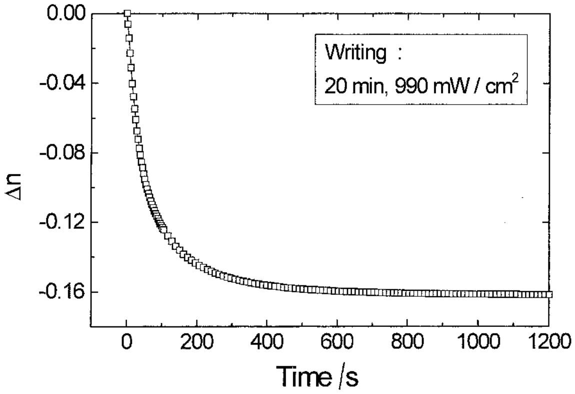

Figure 6. Negative photoinduced birefringence as a function of time; irradiation with 990 mW cm^{-2}.

3. Results and discussion

When irradiated with linearly polarized light, a stable optical birefringence can be induced in an amorphous film of TAM. As mentioned above, the sign of the photoinduced birefringence is negative. Figure 6 shows the time evolution of the negative birefringence using irradiation with a power of 990 mW cm^{-2}.

The writing process leads to remarkably high Δn values of up to 0.16. Yet one has to take into account the fact that the isomerization kinetics of the donor–donor substituted azo chromophores are rather slow. In particular, the thermal *cis-trans* back isomerization is known to be of the order of $k = 4\,\mathrm{e}^{-4}$ for *p,p′*-amino-alkoxy substituted azo dyes [25]. This leads to a relatively high content of *cis*-isomers in the photostationary state (about 30%, when irradiated with 488 nm [26]). The *cis*-species will also contribute to the induced birefringence.

Nevertheless, the photoinduced birefringence was found to be stable and no significant back relaxation of the signal was observed at room temperature during the first hours after switching off the writing beam. Thus, by interference of two s-polarized writing beams one is able to store a stable holographic grating in the TAM material. This is obvious from the growth curve of the grating in terms of the diffraction efficiency shown in figure 7(*a*). Figure 7(*b*) displays, in addition, the polar diagram of the diffraction efficiency as controlled by the photoselection.

Using equations (5) and (6), Δn values were calculated from the diffraction efficiencies. These agree with those of the birefringence measurements within the limits of experimental error. This is a strong indication that the contribution of SRG formation to the overall birefringence in the grating experiment is rather small. However, rotation of the polar diagram by about 8° indicates a coupling of the refractive index grating to a periodical

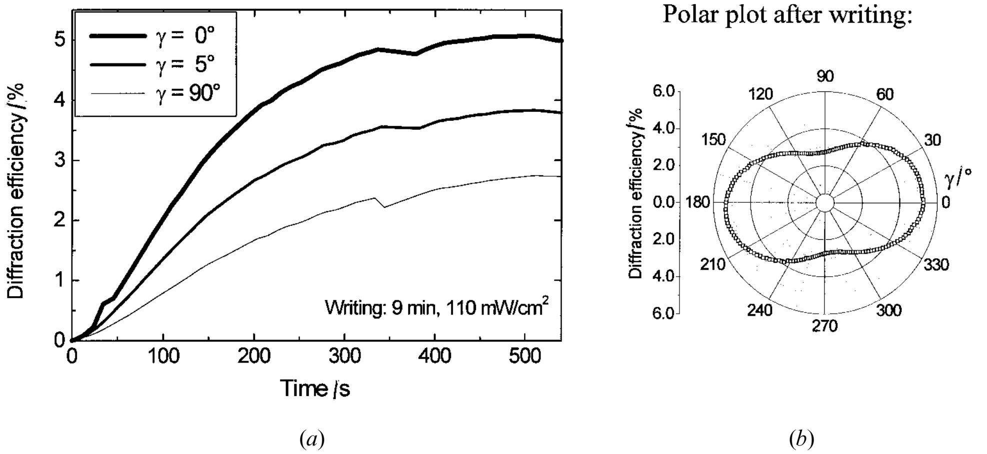

(*a*) (*b*)

Figure 7. (*a*) Holographic growth curve for three different angles of reading beam polarization. (*b*) Polar plot for the angular dependence of the diffraction efficiency.

surface modulation as discussed in [24] and [26], see figure 7(*b*). Indeed, the surface profile analysis gave evidence for weak sinusoidal surface modulations, even when the sample was irradiated with s-polarized beams at medium intensities ($< 500\ \mathrm{mW\,cm^{-2}}$).

3.1. *Thermal treatment*

The efficiency of the photoinduced grating can be raised significantly without any additional irradiation by heating the sample above the glass transition as is obvious from Figure 8.

In the following we will point out the three main characteristic features of the observed effect.

(A) *Region of axis reorientation:* the axis of anisotropy is already turned by nearly 90° before the optical signal increases.
(B) *Region of gain:* the efficiency is raised by up to two orders of magnitude above a temperature of about 80°C.
(C) *Region of gain collapse:* the efficiency rapidly breaks down above a temperature of about 110°C.

It should be mentioned that the observed gain process is dependent on the heating rate: the location of axis reorientation, gain maximum and gain collapse on the temperature scale can be shifted by several Kelvin, but they are reproducible for the same heating conditions.

3.1.1. *Reorientation of the optical axis*

The angular dependence of the diffraction efficiency can be described as follows:

$$\eta(\gamma) = \eta_{\min} + (\eta_{\max} - \eta_{\min}) \cos^2(\gamma - \gamma_0) \qquad (7)$$

where $\eta_{\min}$ and $\eta_{\max}$ are the minimum and maximum efficiencies, respectively. γ_0 denotes the shift angle of maximum efficiency relative to the 0° position. We used this equation to analyse the influence of temperature on the angular dependence of η. For this purpose we recorded a grating at room temperature and determined the efficiency as a function of γ at several temperatures. We evaluated the temperature dependence of the shift angle γ_0 and of the ratio of anisotropy $q_{\mathrm{aniso}} = \eta_{\min}/\eta_{\max}$ by equation (7) to make the fit. The results are plotted in figure 9.

Obviously the axis of anisotropy is not reorientated gradually, but within a small temperature range near 53°C. At the same temperature the anisotropy of the grating increases. As no significant changes of the irradiated surface could be detected after the thermal treatment below 70°C, we speculate that the changes in the anisotropy of the grating are caused by a molecular reorientation of the chromophores. However, temperature dependent measurements of the photoinduced birefringence show no significant changes of Δn and the sign remains negative during the thermal treatment up to 70°C. To judge these results, we have to keep in mind that in the birefringence measurement only the optical

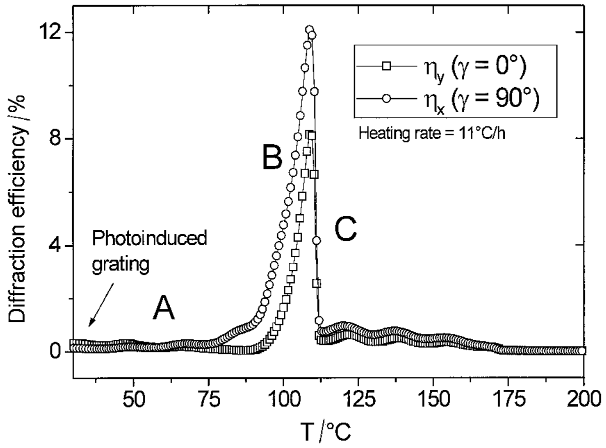

Figure 8. Thermal development of a photoinduced grating (heating rate 11°C h^{-1}).

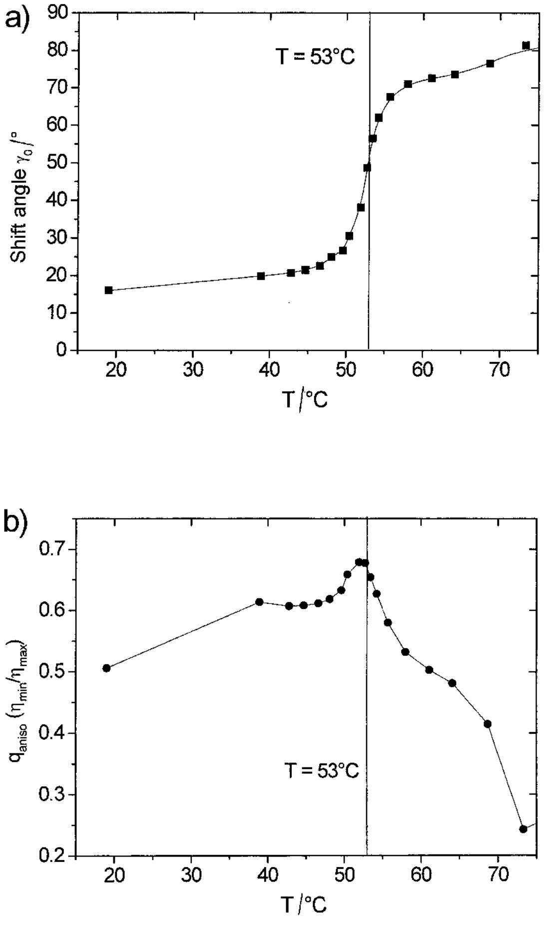

Figure 9. (*a*) Shift angle γ_0 and (*b*) ratio of anisotropy $q_{\mathrm{aniso}} = \eta_{\min}/\eta_{\max}$ of a photoinduced grating as a function of temperature.

changes of the irradiated area are monitored, whereas in the grating experiment both illuminated and dark areas contribute to the detected signal. The possibility of thermally induced reorientation in the non-irradiated areas of the grating will be discussed later.

3.1.2. *Region of gain*

The enhancement of the grating's efficiency can be quantified by defining a gain coefficient *g*. In [27] the gain coefficient is defined as the ratio of the measured efficiencies after writing and thermal treatment. In view of the strong changes of the grating's anisotropy during the gain process, in our case it seemed more appropriate to relate the gain coefficient to the birefringence of the grating:

$$g_{\Delta n} = \frac{\Delta n_{\max}}{\Delta n_{\mathrm{wrt}}}. \quad (8)$$

We investigated the dependence of the initial writing conditions on the amplification of the signal, using equations (5) and (6) to calculate Δn from the measured efficiencies. The gain coefficient is plotted in figure 10 versus the photoinduced Δn of different gratings recorded at room temperature.

After passing a threshold of $\Delta n_{\mathrm{wrt}} = 0.02$, the highest gain coefficient of about $g_{\Delta n} = 10$ will be obtained if the photoinduced grating is far from saturation. As mentioned above, the gain process is dependent on the heating rate and the maximum value of Δn in the gain region can be increased up to 0.5 by using a slow heating rate ($< 20°\mathrm{C\ h^{-1}}$). This value is even higher than expected for a monodomain formation of the calamitic groups and thus cannot be explained only by a reorientational process of the mesogenic chromophores. On the other hand, it is known that the formation of sinusoidal surface modulations will result in a high diffraction efficiency which is far above the saturation level of the refractive index grating [15, 19]. Indeed, we obtained evidence for thermally induced changes of surface modulations by surface profile measurements. We measured the surface of an irradiated sample for this purpose, heated it at a constant heating rate to the temperature of the gain maximum and subsequently froze it in by rapid quenching. The nearly unchanged value of the diffraction efficiency after cooling indicated that no significant changes of the grating occurred during the quenching. Figure 11 shows a comparison of a photoinduced SRG profile and the same grating after the described annealing process.

This experiment gives evidence for a strong amplification of the surface modulation amplitude during the annealing process. In the example considered here the surface depth is changed from 20 nm after writing to 200 nm after the thermal development. The periodicity amounts in both cases to 5 µm. This value thus corresponds to the grating constant of the holographic writing geometry. Strong surface modulations can be achieved even if only a very weak surface grating is produced optically: Figure 12 (*a*) shows the thermally induced increase of the efficiency of a grating with a surface modulation depth of initially less than 5 nm. After the thermal treatment the modulation depth of the remaining grating is found to be more than 400 nm, figure 12 (*b*).

3.1.3. *Collapse of the gain signal*

To understand the sudden breakdown of the gain signal we have to keep in mind that the smectic mesophase is kinetically suppressed in the glassy state of the amorphous prepared film. Temperature dependent birefringence measurements without previous irradiation revealed that the birefringence due to the rearrangements of the liquid crystalline mesogen and the texture formation

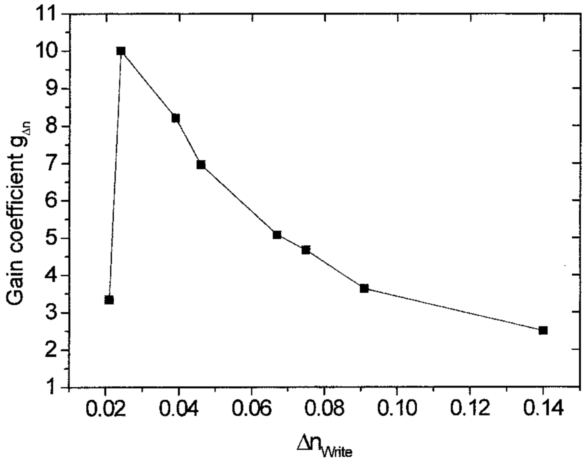

Figure 10. Gain coefficient $g_{\Delta n}$ as a function of the photoinduced birefringence in a holographic grating.

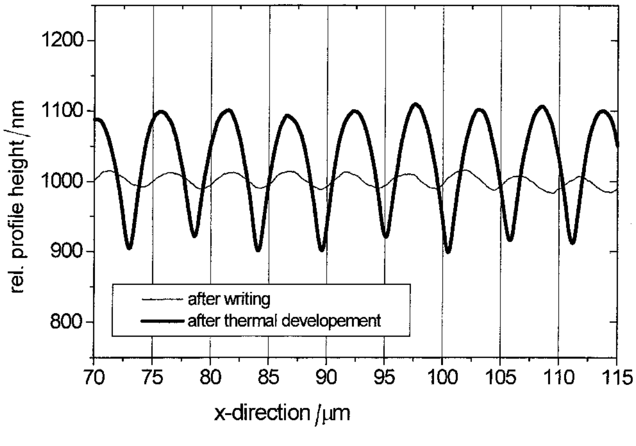

Figure 11. Profile scan of the surface modulation after irradiation and after thermal development into the gain region (curves are shifted horizontally and vertically with respect to each other for better comparison).

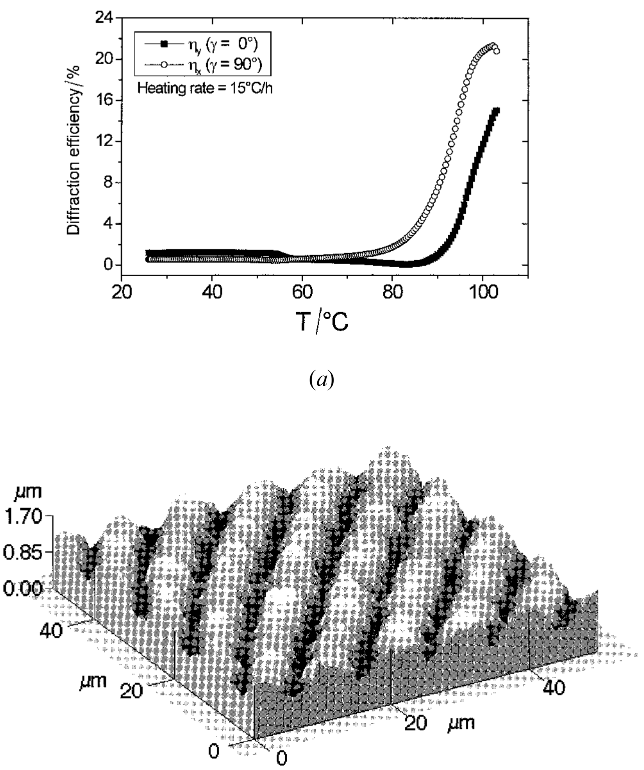

(*a*)

(*b*)

Figure 12. (*a*) Thermal development of a photoinduced grating with only weak surface modulations (< 5 nm); (*b*) AFM image of the irradiated area after thermal treatment.

increases rapidly at about 110°C. At the same temperature, the efficiency of the thermally developed grating and the value of the photoinduced birefringence for a single laser spot irradiation decrease strongly, as can be seen in figure 13.

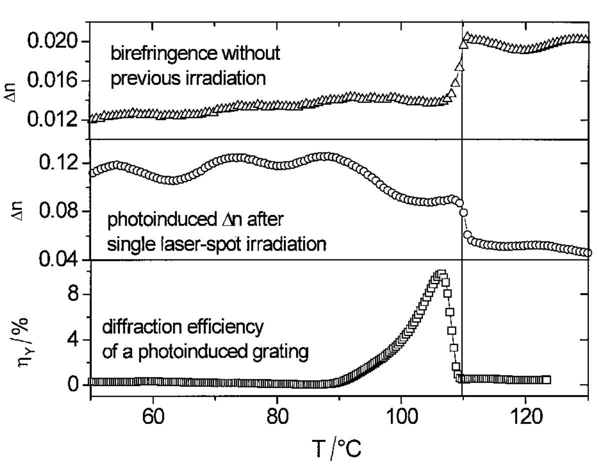

Figure 13. Temperature dependence of the birefringence for an isotropic film (top), for a photo-orientated sample (middle) and of the diffraction efficiency for the case of a grating (bottom).

However, even above 110°C a grating remains with an efficiency comparable to that of the initial photoinduced grating, but with the axis of anisotropy being reoriented. The profile analysis showed a strong irregular modulation of the film surface outside the irradiated area, indicating the formation of ordered domains [28] during the annealing process above 110°C. These findings are in agreement with investigations of Ramanujam *et al.*, who studied the changes of surface modulations and roughness of a low T_g liquid crystalline polyester as a result of ordering processes [29]. Obviously, the orientated chromophores as well as the regular surface modulations are strongly disturbed by the reorganization of the mesogens, giving rise to an increase in film toughness and a partial loss of the macroscopic preferred orientation of the photoaligned groups.

3.2. *Qualitative interpretation of the findings*

The observed thermally induced change of anisotropy of the grating may be explained by a thermally induced reorientational process of the calamitic azo chromophores. Keeping in mind that no change to a positive sign of the photoinduced Δn is observed during heating, we have to exclude an in-plane reorientation of chromophores in the illuminated areas of the grating, as can be shown by considering orientational factors in the photoselection model [9, 30].

Here the isotropic starting condition of the photoselection can be described in this context by the three orientational factors K_x, K_y and K_z:

$$K_x = K_y = K_z = 1/3. \tag{9}$$

Using y-polarized light we obtain for the photoaligned end condition of the illuminated areas:

$$K_y = 0; \quad K_x = K_z = 1/2. \tag{10}$$

The orientational factors can be related to the order parameter S

$$S_i = \frac{3}{2}K_i - \frac{1}{2}, \quad \text{with } i = x, y, z \tag{11}$$

which is proportional to the photoinduced birefringence. So, in principle, the orientational factors can be related to the measured refractive index changes $n_{1,x}$ and $n_{1,y}$ of the grating experiment. Notice that only the relative changes between the orientational factors in the illuminated and in the dark areas contribute to the measured refractive index change, and that no change in the sign of birefringence can be detected by measuring the diffraction efficiency.

Using this concept, the 90° shift of the grating's anisotropy can be explained by a homeotropic rearrangement of chromophores in the non-irradiated areas of the grating. This would lead to the situation that $\eta_y < \eta_x$

and is accompanied by an increase of the anisotropy, as schematically sketched in figure 14(*a*). Figure 14(*b*) shows the corresponding results on the thermally induced change of anisotropy, which fit very well with the qualitative picture. The molecules may be forced into the homeotropic order by the additional volume requirement of the photoinduced isomerization inside the neighbouring irradiated areas. Although such an induced pressure gradient [31, 32] has to exist already during the writing process, the instant reorientation in the dark areas may be restricted for kinetic reasons and it can thus take place only at higher temperatures.

The homeotropic order of the chromophores gives, according to the theoretical models, a good starting point for the formation of strong surface modulations: A high concentration of molecules is characterized by a side-by-side orientation according to the grating vector [17]. The liquid crystalline potential can thus act attractively along the *x*-direction (parallel to the grating vector). It thus supports the migration process which will lead to the formation of surface gratings. Although our arguments can explain the findings at least qualitatively, additional experiments such as SNOM and X-ray analysis must be performed to test our results and obtain a more detailed understanding of this phenomenon.

4. Conclusions

We have demonstrated that the amplification of the contrast of photoinduced gratings by thermal development of a liquid crystalline sample quenched into the amorphous state is due not only to an enhancement of photo-orientation in the LC phase, but is moreover a

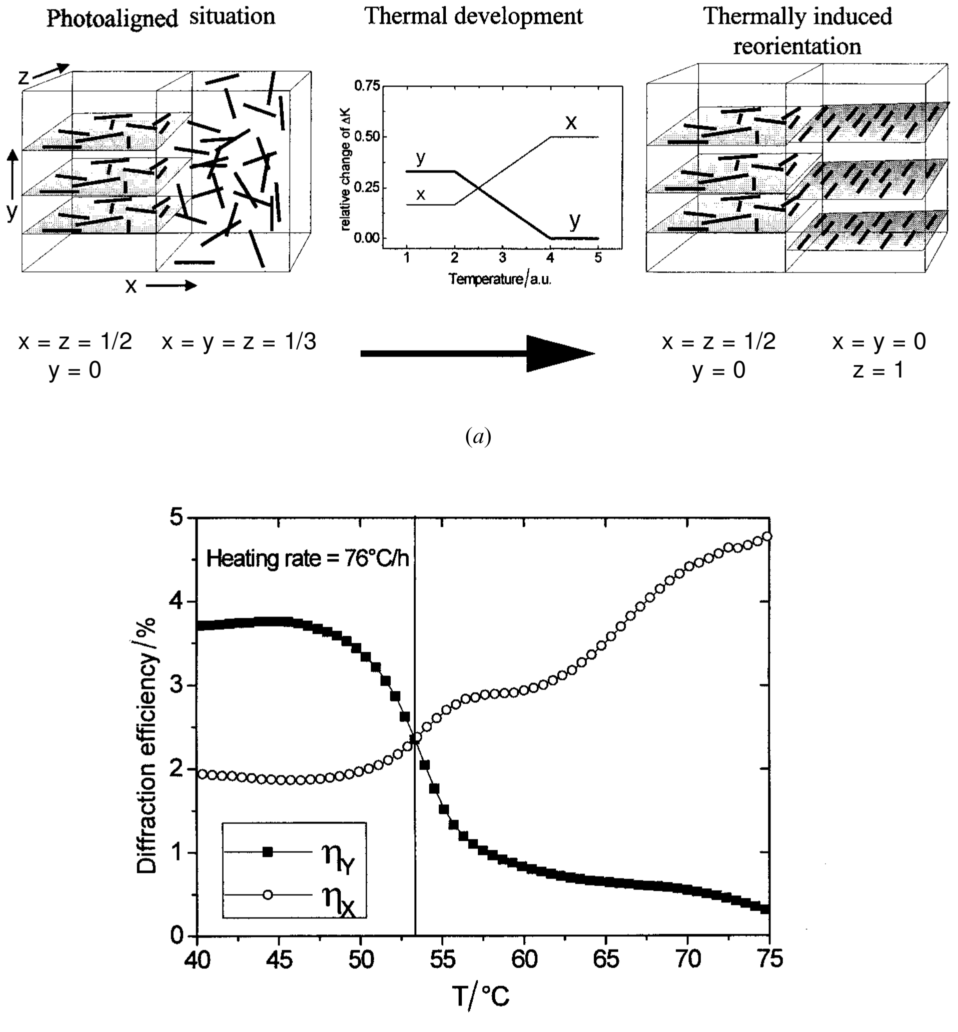

(*a*)

(*b*)

Figure 14. (*a*) Illustration of the thermally induced reorientation of chromophores into the *z*-direction within the non-irradiated regions of the grating and the consequence for the orientational factors. (*b*) Experimental findings for the thermally induced reorientation of the axis of anisotropy of the grating.

consequence of a strong tendency to form surface relief patterns and of their amplification during the thermal treatment. The effect takes place above the glass transition and seems to be controlled by the suppression of the thermotropic phase formation in the glassy state on the one hand and the tendency for mesogenic self-organization due to the liquid crystalline potential on the other hand.

The investigated effect may be used for the development of high efficiency storage materials and optical devices based on liquid crystalline azo compounds. In a primary step, information is written-in optically with low laser exposure and in a second step the contrast of information is amplified strongly by thermal development within the mesophase.

We gratefully acknowledge the financial support by the Deutsche Forschungsgemeinschaft (Ja 668/6-1 and We 496/14-1) and the Fonds der Chemischen Industrie.

References

[1] Eich, M., Wendorff, J. H., Reck, B., and Ringsdorf, H., 1987, *Makromol. Chem. rapid Commun.*, **8,** 59.

[2] Ovanov, S., Yakolev, I., Kostromine, S., Shibaev, V., Laessker, V. L., Stumpe, J., and Kreysig, D., 1991, *Makromol. Chem. rapid Commun.*, **12,** 709.

[3] Petri, A., Kummer, S., and Braeuchle, C., 1995, *Liq. Cryst.*, **19,** 277.

[4] Anderle, K., Birenheide, R., Eich, M., and Wendorff, J. H., 1989, *Makromol. Chem. rapid Commun.*, **10,** 477.

[5] Eich, M., and Wendorff, J. H., 1990, *J. opt. Soc. Am.*, **B7,** 1428.

[6] Anderle, K., and Wendorff, J. H., 1994, *Mol. Cryst. liq. Cryst.*, **51,** 243.

[7] Ivanov, M., Todrov, T., Nikolova, L., Tomova, N., and Dragostinova, V., 1995, *Appl. Phys. Lett.*, **66,** 2174.

[8] Birenheide, R., and Wendorff, J. H., 1990, *Proc. SPIE*, 1213.

[9] Fuhrmann, T., Kunze, M., and Wendorff, J. H., 1998, *Makromol. Theory Simul.*, **7,** 421.

[10] Fischer, T., Läsker, L., and Stumpe, J., 1994, *J. Photochem. Photobiol. A: Chem.*, **80,** 453.

[11] Natansohn, A., Rochon, P., Pèzolet, M., Audet, P., Brown, D., and To, S., 1994, *Macromolecules*, **27,** 2580.

[12] Fischer, T., Läsker, L., Czapla, S., Rübner, J., and Stumpe, J., 1997, *Mol. Cryst., liq. Cryst.*, **298,** 213.

[13] Zilker, S. J., Bieringer, T., Haarer, D., Stein, R. S., van Egmond, J. W., and Kostromine, S., 1998, *Adv. Mat.*, **10,** 855.

[14] Stracke, A., Wendorff, J. H., Janietz, D., and Mahlstedt, S., 1999, *Adv. Mat.*, **11,** 667.

[15] Kim, D. Y., Li, L., Jiang, X. L., Shivshankar, V., Kumar, J., and Tripathy, S. K., 1995, *Macromolecules*, **28,** 8835.

[16] Rochon, P., Batalla, E., and Natansohn, A., 1995, *Appl. Phys. Lett.*, **66,** 136.

[17] Pedersen, T. G., Johannsen, P. M., Holme, N. C. R., Ramanujam, P. S., and Hvilsted, S., 1998, *Phys. Rev. Lett.*, **80,** 89.

[18] Labarthet, F. L., Buffeteau, T., and Sourisseau, C., 1998, *J. phys. Chem. B*, **102,** 2654.

[19] Barrett, C. J., Natansohn, A. L., and Rochon, P. L., 1996, *J. phys. Chem.*, **100,** 8836.

[20] Goldmann, D., Janietz, D., Schmidt, C., and Wendorff, J. H., 1998, *Liq. Cryst.*, **25,** 711.

[21] Holme, N. C. R., Nikolova, L., Ramanujam, P. S., and Hvilsted, S., 1997, *Appl. Phys. Lett.*, **70,** 1518.

[22] Lefin, P., Fiorini, C., and Nunzi, J. M., 1998, *Pure appl. Opt.*, **7,** 71.

[23] Fredericq, E., and Houssier, C., 1973, *Electric Dichroism and Electric Birefringence* (Oxford: Clarendon Press).

[24] Fuhrmann, T., 1997, PhD thesis, Marburg, Germany.

[25] Dubini-Paglia, E., Beltrame, P. L., Marcandalli, B., and Carniti, P., 1986, *J. appl. polym. Sci.*, **31,** 1251.

[26] Stracke, A., 1999, PhD thesis, Marburg, Germany.

[27] Bieringer, T., 1996, PhD thesis, Bayreuth, Germany.

[28] Stettler, A., Hartung, H., Weissflog, W., and Lischka, Ch., 1999, in Proceedings of the 28th Arbeitstagung Flüssigkristalle, Freiburg, P39.

[29] Ramanujam, P. S., Holme, N. C., and Hvilsted, S., 1996, *Appl. Phys. Lett.*, **B68,** 1329.

[30] Michl, J., and Thulstrup, E. W., 1986, *Spectroscopy with Polarized Light* (New York: VCH).

[31] Kumar, J., Li, L., Jiang, X. L., Kim, D. Y., Lee, T. S., and Tripathy, S., 1998, *Appl. Phys. Lett.*, **72,** 2096.

[32] Barrett, C. J., Rochon, P. L., and Natansohn, A., 1998, *J. chem. Phys.*, **109,** 1505.